ARTICLE

An in vitro Förster resonance energy transfer-based high-throughput screening assay identifies inhibitors of SUMOylation E2 Ubc9

Yu-zhe Wang[1,2], Xiao Liu[3], George Way[4], Vipul Madarha[4], Qing-tong Zhou[5], De-hua Yang[1], Jia-yu Liao[4] and Ming-wei Wang[1,2,3]

SUMOylation is one of the posttranslational modifications that mediate cellular activities such as transcription, DNA repair, and signal transduction and is involved in the cell cycle. However, only a limited number of small molecule inhibitors have been identified to study its role in cellular processes. Here, we report a Förster resonance energy transfer (FRET) high-throughput screening assay based on the interaction between E2 Ubc9 and E3 PIAS1. Of the 3200 compounds screened, 34 (1.1%) showed higher than 50% inhibition and 4 displayed dose–response inhibitory effects. By combining this method with a label-free surface plasmon resonance (SPR) assay, false positives were excluded leading to discovering WNN0605-F008 and WNN1062-D002 that bound to Ubc9 with K_D values of 1.93 ± 0.62 and 5.24 ± 3.73 μM, respectively. We examined the effect of the two compounds on SUMO2-mediated SUMOylation of RanGAP1, only WNN0605-F008 significantly inhibited RanGAP1 SUMOylation, whereas WNN1062-D002 did not show any inhibition. These compounds, with novel chemical scaffolds, may serve as the initial material for developing new SUMOylation inhibitors.

Keywords: SUMOylation inhibitor; WNN0605-F008; high-throughput screening; Ubc9; PIAS1; Förster resonance energy transfer; surface plasmon resonance

INTRODUCTION

Posttranslational modifications of proteins, including phosphorylation, acetylation, methylation, and ubiquitination, play important roles in various cellular processes. SUMOylation is an ubiquitin-like posttranslational modification that regulates cellular activities such as transcription, DNA repair, signal transduction, and the cell cycle [1–4]. SUMO (small ubiquitin-like modifier) and ubiquitin share sequence homology and structural similarity but possess different functions. In contrast to ubiquitination, which leads to protein degradation, SUMOylation regulates protein activity, subcellular localization or protein–protein interactions. The SUMO family has five analogs, SUMO1, SUMO2, SUMO3, SUMO4, and SUMO5 [5]. SUMOylation is catalyzed by a multistep enzymatic reaction cascade [5, 6] (Fig. 1). Clearly, protein–protein interactions are crucial for SUMOylation to proceed.

Perturbed SUMOylation contributes to tumorigenesis [7], neurodegeneration [8], and cardiovascular diseases [9]. It is conceivable that SUMOylation processes may be inhibited by small molecules. However, few SUMOylation modulators have been discovered, and no E3 (the SUMO-ligating enzyme) inhibitor has been reported to date [10] (Table 1).

In contrast to the multiple ubiquitin-conjugation enzymes, Ubc9 is the sole E2 (the SUMO-conjugating enzyme) carrier protein and

has no functionally distinct isoforms, which makes it a desirable candidate target for cancer treatment [11]. Ubc9 is associated with the formation, metastasis, and/or poor prognosis of several types of cancer, such as colorectal cancer [12], lung adenocarcinoma [12, 13], liver cancer [14], and melanoma [15]. The functional knockdown of Ubc9 suppressed the estrogen receptor α-dependent signaling pathway in MCF7 breast cancer cells [16]. PIAS1 was initially identified as a "protein inhibitor of activated STAT1" [17] and then was found to function as an E3 ligase through its classic SP-RING domain [18–20]. PIAS1 is involved in tumorigenesis through its positive regulation of oncogenes AKT and MYC [21], as well as negative regulation of tumor suppressors PML, Tp53, and PTEN [22].

Förster resonance energy transfer (FRET) is one of the most accessible methods of studying protein interactions [23]. Quantitative FRET assays are capable of determining various biochemical parameters (e.g., the protein interaction dissociation constant, enzymatic velocity, and K_m) of the SUMOylation machinery and can be used in conjunction with high-throughput screening (HTS) [24–27]. Because of their high efficiency, the FRET pair of CyPet and YPet are often used [28]. Surface plasmon resonance (SPR) is a rapid, real-time, label-free, and sensitive technique to study protein–protein and compound–target interactions [29].

[1]The National Center for Drug Screening and the CAS Key Laboratory of Receptor Research, Shanghai Institute of Materia Medica, Chinese Academy of Sciences (CAS), Shanghai 201203, China; [2]University of Chinese Academy of Sciences, Beijing 100049, China; [3]School of Pharmacy, Shanghai Medical College, Fudan University, Shanghai 200032, China; [4]Department of Bioengineering, Bourns College of Engineering, University of California at Riverside, Riverside, CA 92521, USA and [5]iHuman Institute, ShanghaiTech University, Shanghai 201210, China
Correspondence: De-hua Yang (dhyang@simm.ac.cn) or Jia-yu Liao (jliao@engr.ucr.edu) or Ming-wei Wang (mwwang@simm.ac.cn)

A FRET-based assay identifies SUMOylation E2 Ubc9 inhibitors
YZ Wang et al.

1498

Here, we report the results of an HTS assay based on E2 and E3 interactions to identify novel SUMOylation inhibitors. By combining the FRET with SPR methods, we were able to exclude false positive hits at an early stage and identified WNN0605-F008 as a SUMOylation inhibitor. A chemical library-wide structure similarity search and follow-up bioactivity studies yielded three additional leads, all of which suppressed the SUMOylation of RanGAP1.
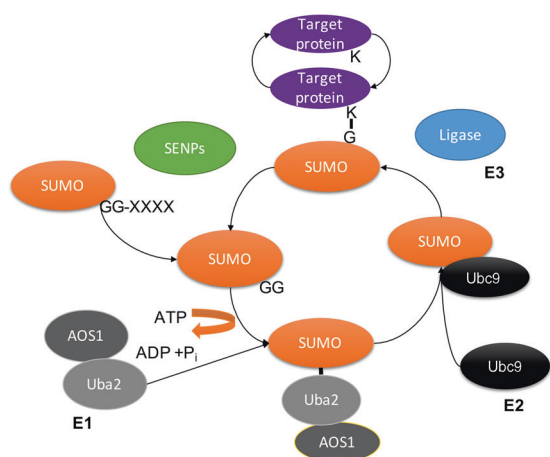

Fig. 1 SUMOylation cascade (i) SUMO precursor is processed by SUMO proteases (SENPs) to expose the C-terminal diglycine; (ii) SUMO forms a thioester-bond with cysteine of E1 enzyme (Aos1/ Uba2 heterodimer) in an ATP-dependent manner [53]; (iii) SUMO is further transferred to the catalytic cysteine (Cys 93) of SUMO-E2 enzyme (Ubc9) [54]; (iv) SUMO forms an isopeptide bond with lysine (ψKxE motif [55]) in the substrate through the function of E2 and E3 enzymes (PIAS, RanBP2 and PC2) [56]; and (v) SUMOylated proteins can be deconjugated by SENPs and SUMO is cleaved off for the next cycle of conjugation.

MATERIALS AND METHODS

Compound library
The compound library (http://www.cncl.org.cn/) used for the FRET-based HTS campaign is a collection of 3200 small molecules from synthetic and natural sources. The structures include lactams, heterocycles, amides, secondary amides, sulfonates, and sulfonamides. These molecules are dissolved in dimethyl sulfoxide (DMSO) at 1 mg/mL (for primary screening) and 5 mg/mL (for secondary screening) stock solutions prior to use.

Reagents
The following reagents were used: DMSO (Sigma-Aldrich, St. Louis, MO, USA), in vitro SUMOylation kits (Abcam, Cambridge, UK), CCK-8 solution (Dojindo, Kumamoto, Japan), RIPA solution (Life Technologies, Carlsbad, CA, USA), protease inhibitor cocktail (Beyotime, Shanghai, China), Ni^{2+}–NTA sepharose beads (GE Healthcare, Chicago, IL, USA), 2D08 and ginkgolic acid (Med-ChemExpress, Monmouth Junction, NJ, USA).
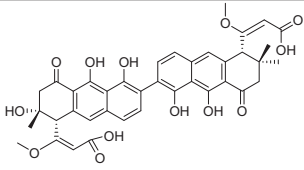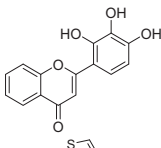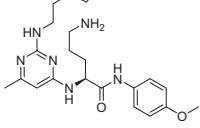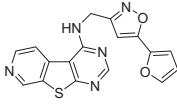
Protein purification
Ubc9 and Cypet–Ubc9 were expressed and purified as previously described [24]. Briefly, pET28b vectors encoding hexa-histidine-tagged recombinant proteins (Ubc9, CyPet–Ubc9, Uba2, Aos1, and PIAS1) were transformed in BL21 (DE3) *Escherichia coli* (*E. coli*) cells. After the cells reached the logarithmic growth phase, 0.1 mM isopropyl beta-*D*-thiogalactoside (IPTG) was added to the medium to induce protein expression at 20 °C (and 180 rpm) for 16 h.

Ypet–PIAS1 was subcloned into a pFastBac1 vector, and recombinant baculoviruses were generated. Sf9 cells (Life Technologies) were cultured at 27 °C (120 rpm) without CO_2 to reach a density of 2×10^6/mL, and then, they were infected with baculovirus and incubated for 72 h. The best multiplicity of infection was determined by a gp64 baculovirus titer kit (PerkinElmer, Boston, MA, USA). Both *E. coli* and Sf9 cells were lysed by sonication.

The hexa-histidine-tagged recombinant proteins were purified by Ni^{2+}–NTA sepharose beads (GE Healthcare) as previously

Table 1. Inhibitors of E2 Ubc9 SUMOylation.

Inhibitor	Target	Substrate	Structure	IC$_{50}$ (µmol/L)	Reference
Spectomycin B1	Ubc9	RanGAP1		4.4	42
2D08	Ubc9	FL-AR peptide		6.0	32
GSK145A	Ubc9	TRPS1 peptide		12.5	45
Compound 2	Ubc9	RanGAP1		75	47

A FRET-based assay identifies SUMOylation E2 Ubc9 inhibitors
YZ Wang et al.

1499

described [26] and eluted in 20 mM Tris-HCl (pH 7.4), 200 mM NaCl and 150 mM imidazole. They were dialyzed and condensed by Amicon Ultra (Merck, Darmstadt, Germany) in 20 mM Tris-HCl (pH 7.4), 50 mM NaCl, and 1 mM dithiothreitol (DTT).

FRET-based HTS campaign
The HTS campaign was carried out in 384-well microtiter plates (PerkinElmer) containing 20 mM Tris-HCl (pH 7.4), 50 mM NaCl, and 1 mM DTT (labeled as FRET buffer). The final concentration of Ypet–PIAS1 and Cypet–Ubc9 used was 1 μM and 1 μM, respectively. Sodium lauryl sulfate, which nonspecifically disrupts protein interactions, was the positive control, since no Ubc9–PIAS1 interaction inhibitor has been reported. Briefly, Cypet–Ubc9 dissolved in FRET buffer (25 μL) was first dispensed with a Bravo liquid handler (Agilent, Santa Clara, CA, USA) to an assay plate followed by the addition of Ypet–PIAS1 (25 μL). After the introduction of compounds (0.5 μL each in 1 mg/mL) to reach a final concentration of 10 μg/mL, ~20 μM, the plates were incubated at room temperature for 30 min, and the fluorescence intensity levels (excitation wavelength (nm)/emission wavelength (nm): 414/530, 414/475, and 475/530) were subsequently measured by an EnSpire® multimode plate reader (PerkinElmer). The initial hit compounds were deliberately selected, dissolved in a 5 mg/mL DMSO solution and rescreened at 10 and 20 μg/mL.

Surface plasmon resonance
We conducted SPR analysis on a Biacore 8K machine with CM5 chips (GE Healthcare) at room temperature. Ubc9 (1 mg/mL) was diluted to 20 μg/mL with acetate buffer (pH 5.0) and immobilized through a standard amine-coupling protocol with an amine-coupling kit (GE Healthcare) to acquire an analyte-binding capacity (R_{max}) of 100 response units (RU). Assuming a 1:1 binding stoichiometry, the immobilized ligand level was calculated with the analyte molecular weight default of 500 Da. The test compounds were serially diluted using Biacore EP+ buffer (GE Healthcare) to eight concentrations that had been predetermined experimentally to obtain the best-fitting kinetics model. Briefly, the analytes passed through chip surface flow cell 1 (fc1) and flow cell 2 (fc2) at a rate of 30 μL/min. The response units were measured in real-time and are shown in the sensor-gram. Both association and dissociation phases were monitored for 120 s, while measurements of the compounds at specific concentrations and a blank (zero concentration) were repeated twice. The experiments were performed in Biacore EP+ buffer (GE Healthcare) consisting of 10 mM HEPES (pH 7.4), 150 mM NaCl, 3 mM EDTA, and 0.005% (v/v) P20. The results were analyzed by Biacore Insight Evaluation (software version 2.0.15.12933). A kinetics rate model using 1:1 binding stoichiometry was employed with nonspecific binding offset by having no Ubc9-conjugate flow cell (fc1) and having a blank control (EP+ buffer).

In vitro SUMOylation
SUMOylation of RanGAP1 was determined by a SUMOylation assay kit (Abcam) following the manufacturer's instructions. We combined all the SUMOylation enzymes (Aos1, Uba2, and Ubc9) and substrates (SUMO2, SUMO3, and RanGAP1), and mixed them thoroughly. Then, we added 1% DMSO or the test compounds (dissolved in DMSO at a final DMSO concentration of 1%). After preincubation with compounds at 37 °C for 10 min, ATP or double-distilled water (for non-ATP groups) was introduced and incubated at 37 °C for 1 h. The reaction was quenched by adding 2× SDS loading buffer (Beyotime), and the samples were boiled at 95 °C for 5 min.

Western blotting
Protein samples were separated by 12% SDS-PAGE gels and transferred onto 0.2-μm Immobilon-P PVDF membranes (Merck). The membranes were blocked with 5% nonfat milk in Tris-buffered saline/Tween-20 (TBST, Epizyme Biotech, Shanghai,

China) for 1 h. The membranes were incubated overnight with primary antibodies at 4 °C, and secondary antibodies were added and incubated for 1 h at room temperature. Membranes were washed three times in TBST and exposed to Western ECL substrate (Bio-Rad, Richmond, CA, USA). Signals were detected by a ChemiDoc™ MP imaging system (Bio-Rad) and analyzed with ImageJ software (National Institutes of Health, Bethesda, MA, USA). The data were normalized to that of the internal control Ubc9 or GAPDH. The SUMOylation percentage was calculated relative to the 1%-DMSO treatment controls. The following antibodies were used: anti-SUMO2/3 (Abcam), anti-Ubc9, anti-SUMO1, anti-GAPDH, and anti-rabbit IgG (Cell Signaling Technology, Danvers, MA, USA).

Library-wide structure similarity search
The similarity search module contained in ActivityBase® software (IDBS, Guildford, UK) was applied to retrieve chemical structures similar to WNN0605-F008 from the 1,792,716 compounds stored in the Chinese National Compound Library (http://www.cncl.org. cn/). The Tanimoto algorithm search approach is based on IDBS ChemXtra cartridge to generate a fingerprint based on the chemical structures stored in the database. The algorithm consists of components referred to the compound composition and structural motifs. Through comparisons of the target structure fingerprints for a query, a Tanimoto coefficient is obtained:

$$T = \frac{NA\&B}{NA + NB - NA\&B}$$

where NA stands for the number of components in the fingerprint of the queried structure, NB stands for the number of components in the fingerprint of the target structure, and NA&B stands for the number of components in the fingerprints of both query and target structures.

Molecular docking
Pose predictions for the hit compounds binding to Ubc9 were performed using Schrodinger Suite 2017-4. A high-resolution (1.8 Å) crystal structure of Ubc9 (PDB code: 2GRN) was prepared using the protein preparation wizard in Maestro 11.4 (Schrodinger, New York, USA) with the default options. The discovered hit compounds and spectomycin B1 were first converted into 3D structures using the LigPrep module in Schrodinger and then docked to Ubc9 with the extra-precision (XP) docking by Glide (Schrodinger). Prime MM-GBSA calculation was performed to consider the induced-fitting effect during ligand-receptor binding, where the residues within 7.0 Å of the ligand were allowed to relax. To identify the potential binding sites, we used SiteMap in Maestro to predict potential binding pockets on the surface of the Ubc9 structures with the Ubc9 active site (as shown in complex with RanGAP1–SUMO1, PDB code: 1Z5S).

SUMOylation of p53 and RanGAP1
A FRET-based SUMOylation assay was conducted with 0.5 μM CyPet-SUMO1 and 2 μM YPet-substrate in the presence of 0.1 μM E1, 0.2 μM E2, and 0.5 μM E3 PIAS1 in SUMOylation buffer (20 mM Tris-HCl, pH 7.5; 50 mM NaCl; 4 mM MgCl2; and 1 mM DTT) in the presence or absence of ATP (negative control) at 37 °C for 60 min. Confirmed hit compounds were introduced individually at a final concentration of 10 μM prior to ATP addition and incubated with all the proteins for 10 min at 22 °C. Absolute FRET signals (Em$_{FRET}$) were used to quantify the inhibitory activity.

Cell culture
HEK293T cells were purchased from American Type Culture Collection and maintained in Dulbecco's modified Eagle's medium (Life Technologies) supplemented with 10% fetal bovine serum (Life Technologies) and 100 units/mL penicillin/streptomycin. They were incubated in a humidified chamber with 5% CO_2 at 37 °C.

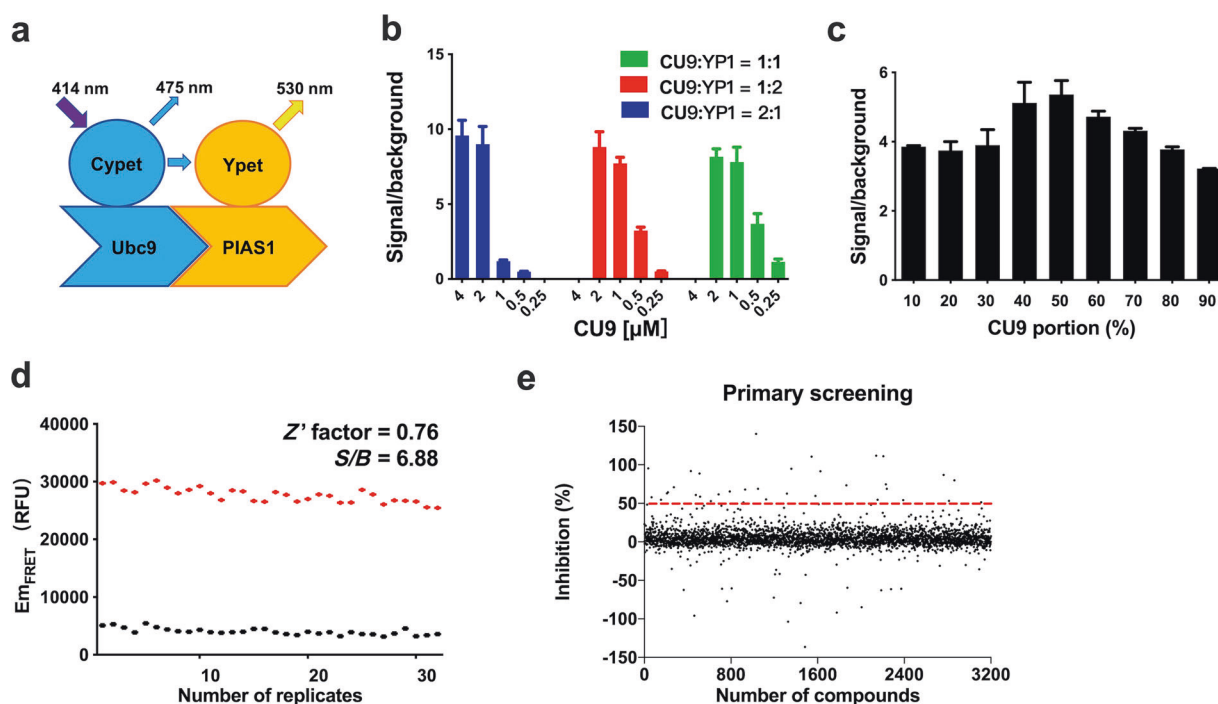A FRET-based assay identifies SUMOylation E2 Ubc9 inhibitors
YZ Wang et al.

1500

Fig. 2 Assay optimization and HTS campaign. a FRET-based detection of Ubc9–PIAS1 interaction (SUMOylation E2 conjugating enzyme and E3 ligase). **b** Signal-to-background (S/B) ratios with different concentrations of Cypet–Ubc9 and Ypet–PIAS1 (n = 3). **c** Signal-to-background (S/B) ratios with different portions of donor Cypet–Ubc9 (n = 3), the total concentration of two proteins is set at 2 μM. **d** Z′ factor of the HTS assay determined under the optimized conditions: 32 signals (negative control, red circles) and 32 blanks (positive control, black circles) were investigated. In the blank group, 40 μM sodium lauryl sulfate was used to block the interaction of two proteins. **e** HTS campaign of 3200 compounds using FRET assay. The results are expressed as percentage of inhibition of EmFRET signal. Dashed line shows the cut off at 50% inhibition.

Cytotoxicity

HEK293T cells were seeded in 96-well plates at a density of 10,000 cells/well. Compounds were added at final concentrations of 100, 50, 25, 12.5, 6.25, and 3.125 μM. DMSO (1%) without inhibitor was used as a nontreated control. The cells were incubated with compounds for 24 h. Ten microliters of CCK-8 solution (Dojindo) was added to each well, and the absorbance at 450 nm was measured by an EnSpire® plate reader (PerkinElmer) after 2 h. Cell viability (%) was evaluated and compared with that of the cells in the nontreated and blank wells.

Baseline SUMOylation

HEK293T cells were cultured in 48-well plates until 80% density was reached. Then, they were treated with 1% DMSO or test compound for 24 h. The cells were then lysed by RIPA solution (Life Technologies) containing protease inhibitor cocktail (Beyotime), and the SUMOylation level was measured by Western blot analysis.

Data analysis

>Dose–response curves and IC_{50} values were generated with the log (inhibitor) vs. response equation used in nonlinear regression analysis. Data are presented as the mean ± SEM of three independent experiments. The significance was evaluated by one-way analysis of variance followed by Bonferroni post hoc test. Differences were considered significant for P values < 0.05. The data analyses were conducted with GraphPad Prism 5 (San Diego, CA, USA). The $Z′$ factor was calculated as follows [30]:

$$Z' = 1 - 3 \times \frac{(\text{SDPC} + \text{SDNC})}{|\text{MPC} - \text{MNC}|},$$

where MPC represents the mean value of the positive control wells; SDPC represents the standard deviation of the positive control wells; MNC represents the mean value of the negative

control wells; and SDNC represents the standard deviation of the negative control wells.

RESULTS

HTS campaign against the Ubc9–PIAS1 interaction
The results are expressed as the percentage of Em_{FRET} signal inhibition. The FRET signal (Em_{FRET}) was calculated as previously described [24] (Fig. 2a). Briefly, a mixture of CyPet–Ubc9 and YPet–PIAS1 was excited at 414 nm, the emission intensity at 530 nm (Em_{total}) consisted of three components: the direct emission of CyPet, the direct emission of YPet, and the sensitized emission of YPet (Em_{FRET} and the true FRET signal). According to the nature of the florescence proteins, the direct emission of CyPet and YPet at 414/530 nm is proportional to their emission peaks (414/475 nm for CyPet and 475/530 nm for Ypet, called FL_{DD} and FL_{AA}, respectively). Hence, the exact FRET signal (Em_{FRET}) can be calculated as follows:

$$Em_{FRET} = Em_{total} - X \times FL_{DD} - Y \times FL_{AA}.$$

By measuring different concentrations of CyPet–Ubc9 alone and YPet–PIAS1 alone, we set $X = 0.378$ and $Y = 0.052$ in our experiments (data not shown).

To optimize the assay with a higher signal-to-background (S/B) ratio, we first adjusted the CyPet–Ubc9 and Ypet–PIAS1 ratio to 1:1 and increased the concentrations of both proteins from 0.25 to 2 μM (Fig. 2b). Under this condition, we varied the portion of CyPet–Ubc9 from 10% to 90%, and the strongest signal was obtained when both CyPet–Ubc9 and Ypet–PIAS1 were at 50% (Fig. 2c). The $Z′$ factor was 0.76 with an S/B ratio of 6.88 (Fig. 2d), indicating that the system was of high quality and well suited to HTS [30]. Fifty percent inhibition was used as the cut-off value for selecting compounds during the primary screening.

A FRET-based assay identifies SUMOylation E2 Ubc9 inhibitors
YZ Wang et al.

1501

Of the 3200 compounds screened (Fig. 2e), 34 (1.1%) showed inhibition >50%. In the secondary screening at two concentrations (10 and 20 μg/mL), 19 compounds displayed consistent inhibitory effects. They were further evaluated in dose–response studies, leading to four confirmed hit compounds with IC$_{50}$ values below 50 μM (Supplementary Fig. S1).

Identification of the Ubc9 inhibitors by SPR

Since some hit compounds (color compounds in particular) may interfere with florescence readouts and cause false positive results [31], we conducted SPR analysis to verify the binding between the hit compounds and target proteins. The Ubc9 inhibitor 2D08 was used as a positive control [32]. WNN0605-F008 and WNN1062-D002 exhibited K_D (equilibrium dissociation constant) values of 1.93 ± 0.62 μM and 5.24 ± 3.73 μM, respectively, whereas the other two hit compounds did not show any binding affinity for Ubc9 (Fig. 3 and Table 2). Notably, WNN0605-F008 and WNN1062-D002 bind to Ubc9 with different kinetics: WNN0605-F008 dissociates slower from Ubc9 ($K_{off} = 3.83 ± 5.14$ ks^{-1}), while WNN1062-D002 associates faster ($K_{on} = 338 ± 252$ mM/s), pointing to different application potential [33].

WNN0605-F008 inhibits SUMOylation of RanGAP1

Ran GTPase-activating protein 1 (RanGAP1) was the first discovered and most abundant SUMOylation substrate in mammals [34]. It is a nuclear trafficking protein, and SUMOylation of RanGAP1 is essential for its nuclear pore localization [35, 36]. SUMO2 is the most abundant SUMO paralog and is regulated in response to stimuli and cell stress [37]. SUMO2 and SUMO3 are 97% identical in structure (indistinguishable by antibodies) and equivalent in function [38, 39]. We studied the effect of the two compounds on SUMO2-mediated SUMOylation of RanGAP1 using ginkgolic acid (E1, the SUMO-activating enzyme inhibitor) as a positive control [40]. Only WNN0605-F008 significantly inhibited RanGAP1 SUMOylation (Fig. 4), whereas 2D08 bound to Ubc9 (Fig. 3b) and suppressed IκBα and topoisomerase-I regulated SUMOylation [32]. This may suggest different binding sites and substrate selectivity between 2D08 and WNN0605-F008. WNN1062-D002 did not induce any inhibition, which might have been due to its rapid dissociation kinetics or affinity for a different binding site, a possibility worthy of further investigation.
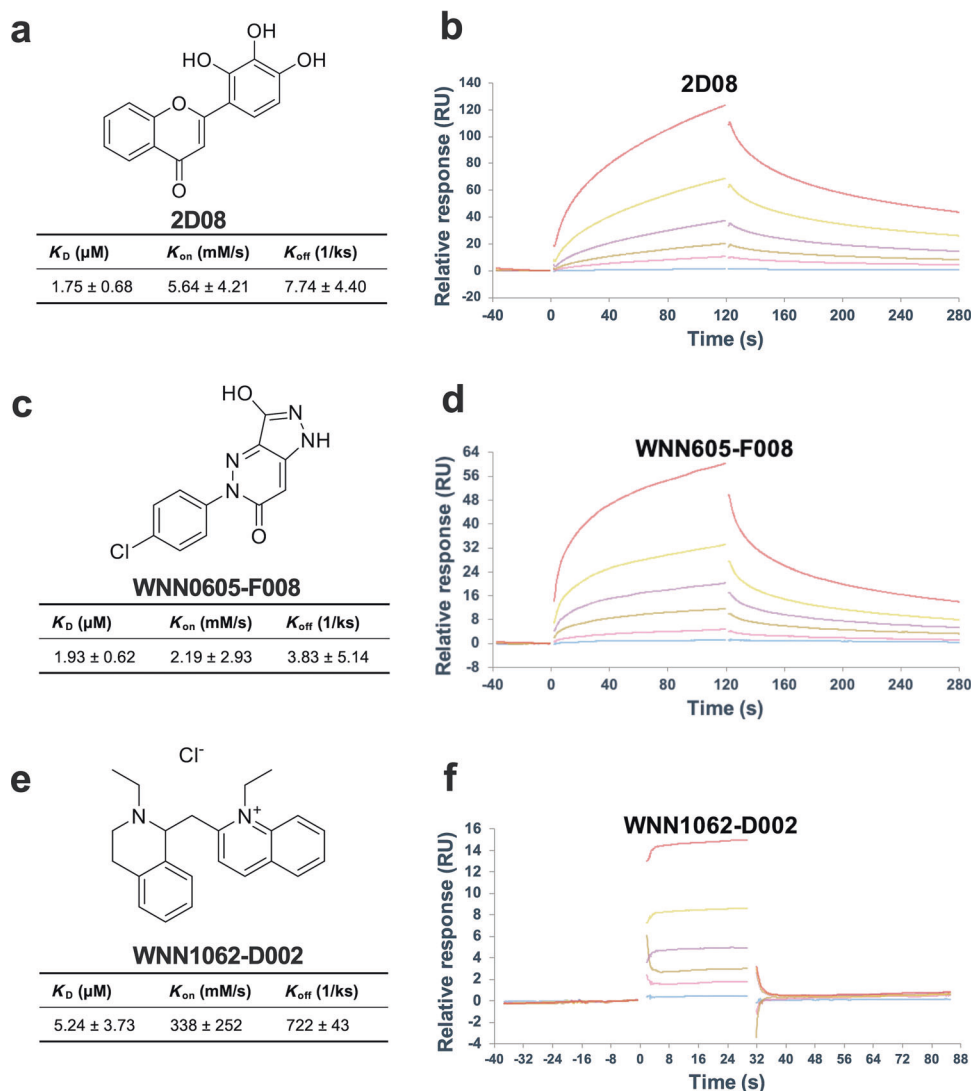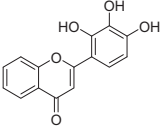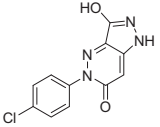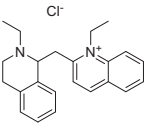

a, b Structure and kinetics of 2D08

2D08		
K_D (μM)	K_{on} (mM/s)	K_{off} (1/ks)
1.75 ± 0.68	5.64 ± 4.21	7.74 ± 4.40

WNN0605-F008		
K_D (μM)	K_{on} (mM/s)	K_{off} (1/ks)
1.93 ± 0.62	2.19 ± 2.93	3.83 ± 5.14

WNN1062-D002		
K_D (μM)	K_{on} (mM/s)	K_{off} (1/ks)
5.24 ± 3.73	338 ± 252	722 ± 43

Fig. 3 **Surface plasmon resonance analysis shows that WNN0605-F008 and WNN1062-D002 bound to Ubc9 with different kinetics.** **a, b** Structure and kinetics of 2D08 (positive control, $K_D = 1.75 ± 0.68$ μM). **c, d** Structure and kinetics of WNN0605-F008. WNN0605-F008 ($K_D = 1.93 ± 0.62$ μM) exhibits a slow association and disassociation pattern for Ubc9. **e, f** Structure and kinetics of WNN1062-D002. WNN1062-D002 ($K_D = 5.24 ± 3.73$ μM) displays a quick association and disassociation pattern for Ubc9. Compound concentrations were 10, 5, 2.5, 1.25, 0.625, and 0.078 μM in descending order. RU response units.

A FRET-based assay identifies SUMOylation E2 Ubc9 inhibitors
YZ Wang et al.

1502

Table 2. Structures and K_D values of confirmed hits.

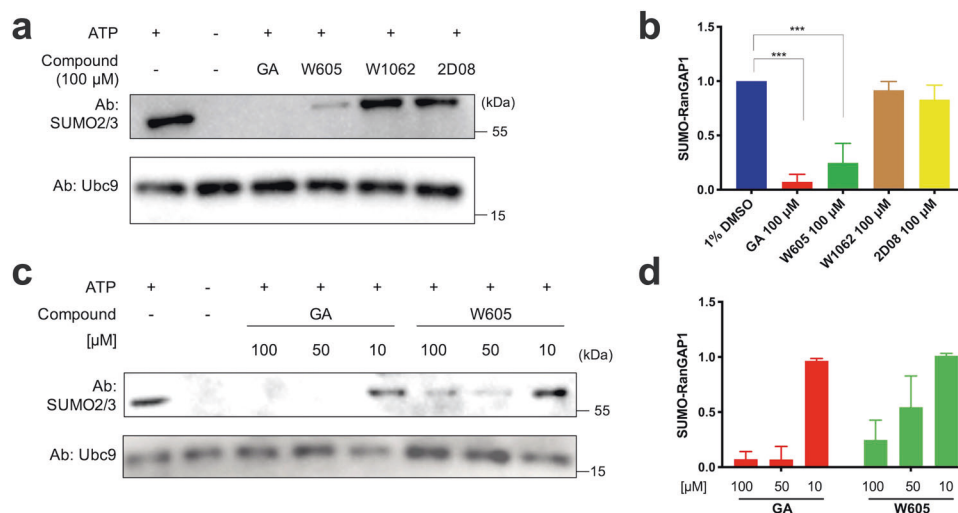| Compound	Formula	Structure	Molecular weight	K_D (μM)	K_{on} (mM/s)	K_{off} (1/ks)	CAS number
2D08	$C_{15}H_{10}O_4$		270.24	1.75 ± 0.68	5.64 ± 4.21	7.74 ± 4.40	144707-18-6
WNN0605-F008	$C_{11}H_7ClN_4O_2$		262.65	1.93 ± 0.62	2.19 ± 2.93	3.83 ± 5.14	338418-81-8
WNN1062-D002	$C_{23}H_{23}ClN_2$		362.90	5.24 ± 3.73	338 ± 252	722 ± 43	1101191-45-0

Fig. 4 Inhibition of SUMOylation by WNN0605-F008. a, b WNN0605-F008 (W605) reduced RanGAP1 SUMOylation. Inhibition of SUMO2-RanGAP1 after treatment ($n = 3$). Protein levels were normalized to Ubc9. **c, d** WNN0605-F008 (W605) reduced SUMO2-RanGAP1 in three different concentrations. ***$P < 0.001$. GA ginkgolic acid; Ab antibody.

Library-wide similarity search for WNN0605-F008 analogs

Based on the structure of WNN0605-F008, 121 samples from the 1,792,716 compound collection were identified with Tanimoto coefficients higher than 80 (Fig. 5a). We first performed the default "LMW screening" method on the 121 compounds with a Biacore 8 K machine (data not shown) followed by a "LMW multicycle kinetics" evaluation on those compounds showing significant binding affinities (RU). Three hit compounds that bind to Ubc9 at the micromolar K_D levels (Supplementary Fig. S2 and Table 3) were obtained, and all of them (WNN0362-H004, WNN0603-B003, and WNN2089-D007) inhibited RanGAP1 SUMOylation in a dose-dependent manner (Fig. 5b).

Computational analysis of the binding modes of the confirmed hit compounds

To understand the molecular basis of the inhibitory activity of the confirmed hit compounds, we performed molecular docking studies on the basis of high-resolution Ubc9 crystal structure (1.8

Å, PDB:2GRN). To discover the potential binding sites in Ubc9 for these compounds using SiteMap, we found that spectomycin B1 had a better docking score and formed stronger interactions within the active site of Ubc9 (Fig. 6a), while 2D08 preferentially bound to the allosteric site (Glu42 and Lys59) of Ubc9 (Supplementary Fig. S3) [41]. One carboxyl end of spectomycin B1 formed salt bridges with Arg104, and another carboxyl end formed hydrogen bonds with Asn124 and Ser95. In addition, the naphthalene rings of spectomycin B1 were stabilized upon forming hydrophobic contacts with Leu94, Ile96, and Leu119 and cation–π interactions with Arg104 (Fig. 6). WNN0605-F008 and WNN0362-H004 were predicted to occupy the catalytic pocket of Ubc9. WNN0605-F008 formed hydrogen bonds with Ser95, Lys101, and Asp127, and the benzene ring formed additional hydrophobic interactions with Leu94 and Leu119. Similarly, WNN0362-H004 formed hydrogen bonds with Cys93, Ser96, Glu98, and Asp127. Given the nature of the catalytic site of Ubc9, spectomycin B1, WNN0605-F008, and WNN0362-H004 were expected to directly
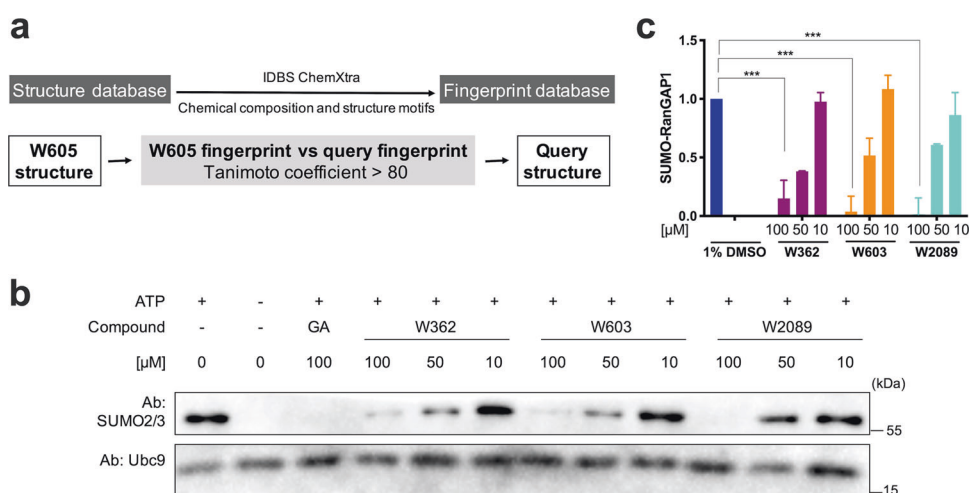
A FRET-based assay identifies SUMOylation E2 Ubc9 inhibitors
YZ Wang et al.

1503

Fig. 5 **Structure similarity check and Ubc9 binding screening. a** Workflow of similarity check. **b** SUMOylation inhibition by WNN0362-H004 (W362), WNN0603-B003 (W603), and WNN02089-D007 (W2089) in three different concentrations. **c** Inhibition of SUMO2-RanGAP1 after treatment ($n = 3$). Protein levels were normalized to Ubc9. ***$P < 0.001$. GA ginkgolic acid; Ab antibody.

Table 3. Structures and K_D values of bioactive WNN0605-F008 analogs.

Compound	Formula	Structure	Molecular weight	K_D (µM)	K_{on} (mM/s)	K_{off} (1/ks)	CAS number
WNN0605-F008	$C_{11}H_7ClN_4O_2$		262.65	1.93 ± 0.62	2.19 ± 2.93	3.83 ± 5.14	338418-81-8
WNN0362-H004	$C_{11}H_{12}N_6O_2$		260.25	82.09 ± 23.72	0.11 ± 0.09	7.83 ± 4.80	129109-53-1
WNN0603-B003	$C_{17}H_{14}N_4O_3$		322.32	13.32 ± 0.45	0.32 ± 0.26	4.33 ± 3.63	338405-08-6
WNN2089-D007	$C_{16}H_{12}ClN_3O_3$		329.74	14.94 ± 13.52	0.29 ± 0.26	2.38 ± 0.03	341955-88-2

affect the catalytic activity of Ubc9, which would be consistent with our functional studies (Figs. 4 and 5) and the published data [42]. In addition, 2D08 did not fit the catalytic pocket, which may explain the negative results for the RanGAP1 SUMOylation assay (Fig. 4a). Inhibition of IκBα and topo-I SUMOylation [32] may have resulted from an allosteric effect (Supplementary Fig. S3).

Substrate preference of the confirmed hit compounds
We further evaluated the effect of four confirmed hit compounds on two SUMOylation substrates, p53 and RanGAP1. At a relatively low concentration (10 µM), they inhibited SUMOylation when p53 was used as the substrate (Fig. 6b). Compounds WNN0362-H004 and WNN0603-B003, but not WNN0605-F008 or WNN2089-D007, exhibited weaker inhibitory activity when RanGAP1 was used (Fig. 6c), suggesting that E2 Ubc9 and E3 PIAS1 may play diverse roles in facilitating the transfer of the SUMO peptide to different substrates.

Effects of the hit compounds in vitro
The cytotoxicity of the hit compounds was tested in HEK293T cells using the CCK-8 assay. With maximum 100 µM compound exposure, the reduction in cell viability was <25% for each compound (Supplementary Fig. S4c). The inhibitors were also investigated for their effects on HEK293T baseline SUMOylation. Following a 24-h compound incubation, SUMOylation was detected by Western blotting. SUMO1 and SUMO2/3 modifications were unaffected in the HEK293T cells (Supplementary Fig. S4a, b). Insufficient intracellular concentrations may lead to poor effects in cells.

DISCUSSION

SUMOylation plays an essential role in cellular processes and diseases. However, only a limited number of small molecule inhibitors have been identified to date. In this study, we present
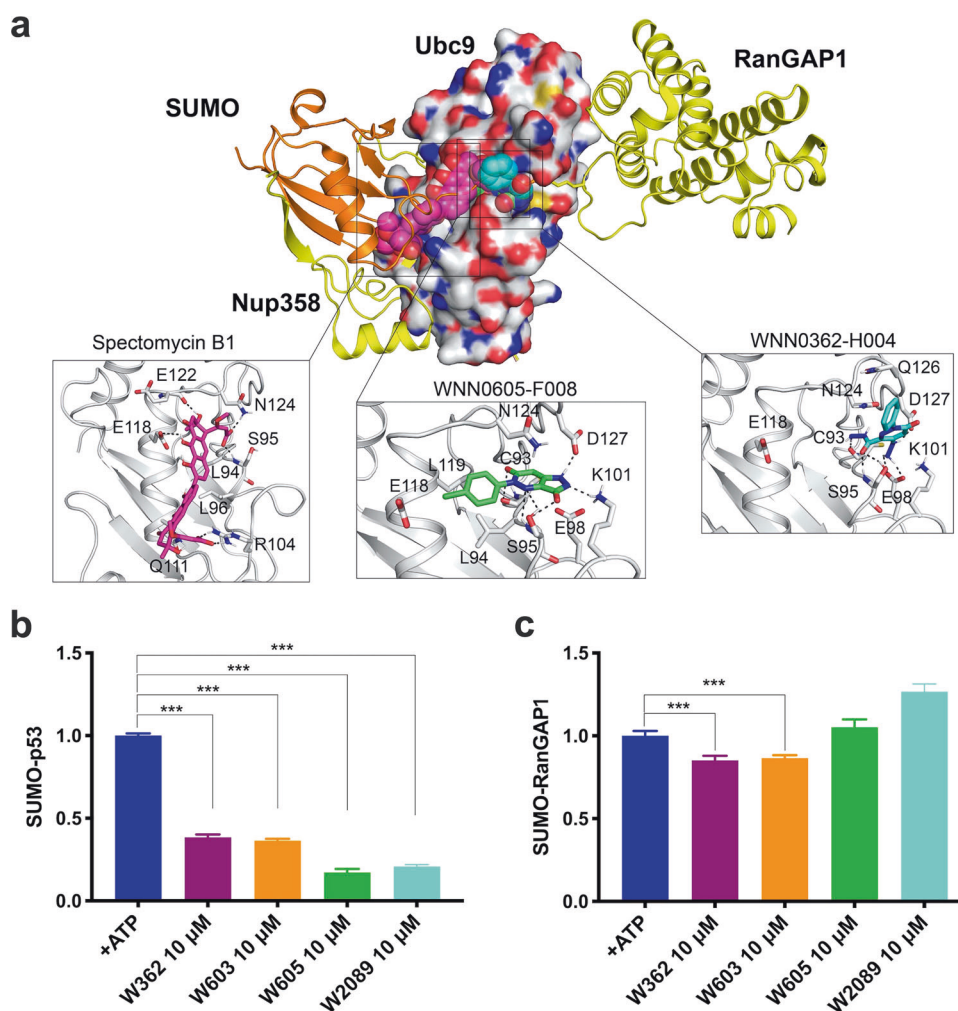
A FRET-based assay identifies SUMOylation E2 Ubc9 inhibitors
YZ Wang et al.

1504

Fig. 6 Binding modes and substrate preference of confirmed hits. a Catalytic pocket of UBC9 and predicted poses of spectomycin B1, WNN0605-F008, and WNN0362-H004. Ubc9 is shown as surface, and its binding partners SUMO1, RanGAP1, and Nup358 are shown in cartoon (PDB code: 1Z5S). The carbon atoms of spectomycin B1, WNN0362-H004, and WNN0605-F008 are colored in magenta, green, and cyan, respectively. The image was generated using PyMOL 2.1. **b** SUMOylation of p53 is inhibited by WNN0362-H004 (W362), WNN0603-B003 (W603), WNN0605-F008 (W605), and WNN2089-D007 (W2089) in the FRET assay. **c** SUMOylation of RanGAP1 is inhibited by WNN0362-H004 (W362) and WNN0603-B003 (W603) in the FRET assay. ***$P < 0.001$.

the outcome of a FRET-based HTS campaign employed to discover small molecule inhibitors of protein interactions within the SUMOylation machinery. Instead of using the entire SUMOylation system, we extracted two main enzymes (Ubc9 and PIAS1) to simplify the screening process. The assay system was optimized to maximize the S/B ratio based on changes in the concentrations of Ubc9 and PIAS1. The primary screening results were verified by SPR, a label-free and sensitive binding detection approach, to eliminate false positives. The hit rate was improved by a library-wide similarity search for WNN0605-F008 analogs, which yielded three additional inhibitors of SUMOylation (acting against E2 Ubc9).

Förster (or fluorescence) resonance energy transfer (FRET), a fast, adaptable and real-time method, has been widely used in biochemistry and cell biology studies. As a spectroscopic ruler, it is effective in the 1–10 nm range. The instrumentation for FRET assays is accessible to most laboratories, and diverse FRET pairs (e.g., CFP-YFP, GFP-RFP, or FFP-IFP) are readily available. However, unlike time-resolved FRET, classical FRET is rarely used in drug screening [26]. Some attempts using quantum dot FRET did not lead to desirable outcomes, but our work indicates the possibility of using FRET for HTS drug screening.

As proteomics and genetic screening technologies are advancing rapidly, an increasing number of SUMOylation substrates (including transcription factors, replication factors, transport factors, virus proteins and cytoskeleton components) have been identified [43, 44]. The basic mechanisms of SUMOylation are relatively well defined. However, the substrate recognition specificity remains unclear. Known Ubc9 inhibitors showed selective activity toward substrates (Table 1). The 2D08 compound was found in an electrophoretic mobility shift assay using a synthesized fluorescent peptide derived from the androgen receptor. It was shown to inhibit SUMOylation of IκBα and topo-I [32]. GSK145A was discovered with a high-throughput fluorescence polarization assay using a peptide containing the lys1201 SUMOylation site TRPS1. It was demonstrated to inhibit the SUMOylation of the TRPS1 peptide [45]. Spectomycin B1 was found through an in situ cell-based screening system using RanGAP1. It was observed to inhibit the SUMOylation of RanGAP1, p53, and the estrogen-dependent proliferation of MCF7 breast cancer cells [42, 46]. Compound 2 was revealed via a small molecule microarray-based screening using fluorescently tagged Ubc9. It was observed to inhibit the SUMOylation of RanGAP1 [47]. New inhibitors of Ubc9 can be used as chemical probes to further

A FRET-based assay identifies SUMOylation E2 Ubc9 inhibitors
YZ Wang et al.

1505

investigate the detailed mechanism of substrate selectivity and binding dynamics of substrates.

Compared with 2D08, the four compounds found in this study bind directly to Ubc9 but show different kinetics and substrate selectivity [32], which may indicate different mechanisms of action. Of interest is that two of the confirmed hit compounds (WNN0362-H004 and WNN0603-B003) were less inhibitory when the substrate was RanGAP1 (as opposed to p53). Such a substrate preference is consistent with previously published data showing that interferon γ-targeting genes were differentially affected in PIAS-knockout mice [48]. Ubc9 directly binds the SUMO consensus motif and primarily defines substrate specificity [49]. Nonetheless, the PIAS protein is required for efficient SUMO transfer of some substrates. Comprehensive structural studies of the SUMO-E2–E3-substrate quaternary complex will provide valuable insights into this substrate-selective mechanism.

To date, two active sites in Ubc9 have been reported: the catalytic active site (Cys93–Asp127) [50] and the allosteric site (Glu42–Lys59) [41]. We thus performed molecular docking studies on the hit compounds and hypothesized that WNN0605-F008 binds to the catalytic active site (Cys93–Asp127), while 2D08 binds to the allosteric site (Fig. 6 and Supplementary Fig. S3). Both WNN0605-F008 and spectomycin B1 inhibited RanGAP1 SUMOylation [42], while 2D08 was inactive toward RanGAP1. This led to our hypothesis suggesting that the catalytic active site in Ubc9 functions in RanGAP1 SUMOylation, while the allosteric site in Ubc9 functions in IκBα SUMOylation. Further studies using Ubc9 mutations and different substrates are needed to better understand the mechanism of substrate specificity.

Although these confirmed hit compounds may be used as initial leads in drug discovery, their precise mechanism of action, as well as their efficacy in vivo, are unclear. In the canonical interface of ubiquitin RING-type E3 and E2 enzymes, specific residues within the SP-RING domain in PIAS1 contact the L4 loop in Ubc9 [51]. Obviously, affinity pull-down or immunoprecipitation approaches using endogenous or artificial expression systems would be useful for identifying the molecular targets associated with these hit compounds.

Notably, the compounds reported here are of low molecular weight (~300 Da), which makes them chemical fragments. Therefore, their activities can be further improved by fragment-based drug design methods [52].

In summary, we have developed a FRET-based assay to measure the interaction between Ubc9 and PIAS1. It was used to screen potential inhibitors in 384-well plates, and the resultant hit compounds were verified by label-free SPR and in vitro SUMOylation methods. Additional hit compounds were subsequently obtained via a library-wide structure similarity search of WNN0605-F008 analogs. This new scaffold may serve as a starting point for chemical modification and structure-activity relationship studies.

AUTHOR CONTRIBUTIONS
MWW and JYL conceived the idea. MWW, JYL, DHY, YZW, and GW designed the study. YZW, XL, GW, VM and QTZ performed the experiments. YZW, QTZ, JYL, and MWW analyzed the data and wrote the paper.

ADDITIONAL INFORMATION
The online version of this article (https://doi.org/10.1038/s41401-020-0405-7) contains supplementary material, which is available to authorized users.

Competing interests: The authors declare no competing interests.

REFERENCES
1. Guo C, Henley JM. Wrestling with stress: roles of protein sumoylation and desumoylation in cell stress response. IUBMB Life. 2014;66:71–7.
2. Ulrich HD. Ubiquitin and SUMO in DNA repair at a glance. J Cell Sci. 2012;125:249–54.
3. Vertegaal AC, Srikumar T, Lee C, Osula O, Subramonian D, Zhang XD, et al. A proteomic study of SUMO-2 target proteins. J Biol Chem. 2004;279:33791–8.
4. Li T, Evdokimov E, Shen RF, Chao CC, Tekle E, Wang T, et al. Sumoylation of heterogeneous nuclear ribonucleoproteins, zinc finger proteins, and nuclear pore complex proteins: a proteomic analysis. Proc Natl Acad Sci USA. 2004;101:8551–6.
5. Geiss-Friedlander R, Melchior F. Concepts in sumoylation: a decade on. Nat Rev Mol Cell Biol. 2007;8:947–56.
6. Johnson ES. Protein modification by SUMO. Annu Rev Biochem. 2004;73:355–82.
7. Seeler JS, Dejean A. SUMO and the robustness of cancer. Nat Rev Cancer. 2017;17:184–97.
8. Krumova P, Weishaupt JH. Sumoylation in neurodegenerative diseases. Cell Mol Life Sci. 2013;70:2123–38.
9. Mendler L, Braun T, Muller S. The ubiquitin-like SUMO system and heart function: from development to disease. Circ Res. 2016;118:132–44.
10. Licciardello MP, Kubicek S. Pharmacological treats for SUMO addicts. Pharmacol Res. 2016;107:390–7.
11. Mo YY, Moschos SJ. Targeting Ubc9 for cancer therapy. Expert Opin Ther Targets. 2005;9:1203–16.
12. Moschos SJ, Jukic DM, Athanassiou C, Bhargava R, Dacic S, Wang X, et al. Expression analysis of Ubc9, the single small ubiquitin-like modifier (SUMO) E2 conjugating enzyme, in normal and malignant tissues. Hum Pathol. 2010;41:1286–98.
13. McDoniels-Silvers AL, Nimri CF, Stoner GD, Lubet RA, You M. Differential gene expression in human lung adenocarcinomas and squamous cell carcinomas. Clin Cancer Res. 2002;8:1127–38.
14. Tomasi ML, Tomasi I, Ramani K, Pascale RM, Xu J, Giordano P, et al. S-adenosyl methionine regulates ubiquitin-conjugating enzyme 9 protein expression and sumoylation in murine liver and human cancers. Hepatology. 2012;56:982–93.
15. Moschos SJ, Smith AP, Mandic M, Athanassiou C, Watson-Hurst K, Jukic DM, et al. SAGE and antibody array analysis of melanoma-infiltrated lymph nodes: identification of Ubc9 as an important molecule in advanced-stage melanomas. Oncogene. 2007;26:4216–25.
16. Mo YY, Yu Y, Ee PL, Beck WT. Overexpression of a dominant-negative mutant Ubc9 is associated with increased sensitivity to anticancer drugs. Cancer Res. 2004;64:2793–8.
17. Liu B, Liao J, Rao X, Kushner SA, Chung CD, Chang DD, et al. Inhibition of Stat1-mediated gene activation by PIAS1. Proc Natl Acad Sci USA. 1998;95:10626–31.
18. Johnson ES, Gupta AA. An E3-like factor that promotes SUMO conjugation to the yeast septins. Cell. 2001;106:735–44.
19. Kahyo T, Nishida T, Yasuda H. Involvement of PIAS1 in the sumoylation of tumor suppressor p53. Mol Cell. 2001;8:713–8.
20. Kotaja N, Karvonen U, Janne OA, Palvimo JJ. PIAS proteins modulate transcription factors by functioning as SUMO-1 ligases. Mol Cell Biol. 2002;22:5222–34.
21. Rabellino A, Melegari M, Tompkins VS, Chen W, Van Ness BG, Teruya-Feldstein J, et al. PIAS1 promotes lymphomagenesis through MYC upregulation. Cell Rep. 2016;15:2266–78.
22. Rabellino A, Andreani C, Scaglioni PP. The role of PIAS SUMO E3-ligases in cancer. Cancer Res. 2017;77:1542–7.
23. Liao JY, Song Y, Liu Y. A new trend to determine biochemical parameters by quantitative FRET assays. Acta Pharmacol Sin. 2015;36:1408–15.
24. Song Y, Madahar V, Liao J. Development of FRET assay into quantitative and high-throughput screening technology platforms for protein-protein interactions. Ann Biomed Eng. 2011;39:1224–34.
25. Liu Y, Song Y, Madahar V, Liao J. Quantitative förster resonance energy transfer analysis for kinetic determinations of SUMO-specific protease. Anal Biochem. 2012;422:14–21.
26. Song Y, Liao J. An in vitro förster resonance energy transfer-based high-throughput screening assay for inhibitors of protein-protein interactions in Sumoylation pathway. Assay Drug Dev Technol. 2012;10:336–43.

1506

27. Wiryawan H, Dan K, Etuale M, Shen Y, Liao J. Determination of SUMO1 and ATP affinity for the SUMO E1 by quantitative FRET technology. Biotechnol Bioeng. 2015;112:652–8.

28. Nguyen AW, Daugherty PS. Evolutionary optimization of fluorescent proteins for intracellular FRET. Nat Biotechnol. 2005;23:355–60.

29. Fivash M, Towler EM, Fisher RJ. Biacore for macromolecular interaction. Curr Opin Biotechnol. 1998;9:97–101.

30. Zhang JH, Chung TD, Oldenburg KR. A simple statistical parameter for use in evaluation and validation of high throughput screening assays. J Biomol Screen. 1999;4:67–73.

31. Baell JB, Holloway GA. New substructure filters for removal of pan assay interference compounds (PAINS) from screening libraries and for their exclusion in bioassays. J Med Chem. 2010;53:2719–40.

32. Kim YS, Nagy K, Keyser S, Schneekloth JS Jr. An electrophoretic mobility shift assay identifies a mechanistically unique inhibitor of protein sumoylation. Chem Biol. 2013;20:604–13.

33. Vauquelin G. Effects of target binding kinetics on in vivo drug efficacy: koff, kon and rebinding. Br J Pharmacol. 2016;173:2319–34.

34. Matunis MJ, Coutavas E, Blobel G. A novel ubiquitin-like modification modulates the partitioning of the Ran-GTPase-activating protein RanGAP1 between the cytosol and the nuclear pore complex. J Cell Biol. 1996;135:1457–70.

35. Mahajan R, Gerace L, Melchior F. Molecular characterization of the SUMO-1 modification of RanGAP1 and its role in nuclear envelope association. J Cell Biol. 1998;140:259–70.

36. Mahajan R, Delphin C, Guan T, Gerace L, Melchior F. A small ubiquitin-related polypeptide involved in targeting RanGAP1 to nuclear pore complex protein RanBP2. Cell. 1997;88:97–107.

37. Tempe D, Piechaczyk M, Bossis G. SUMO under stress. Biochem Soc Trans. 2008;36:874–8.

38. Saitoh H, Hinchey J. Functional heterogeneity of small ubiquitin-related protein modifiers SUMO-1 versus SUMO-2/3. J Biol Chem. 2000;275:6252–8.

39. Tatham MH, Jaffray E, Vaughan OA, Desterro JM, Botting CH, Naismith JH, et al. Polymeric chains of SUMO-2 and SUMO-3 are conjugated to protein substrates by SAE1/SAE2 and Ubc9. J Biol Chem. 2001;276:35368–74.

40. Fukuda I, Ito A, Hirai G, Nishimura S, Kawasaki H, Saitoh H, et al. Ginkgolic acid inhibits protein sumoylation by blocking formation of the E1-SUMO intermediate. Chem Biol. 2009;16:133–40.

41. Hewitt WM, Lountos GT, Zlotkowski K, Dahlhauser SD, Saunders LB, Needle D, et al. Insights into the allosteric inhibition of the SUMO E2 enzyme Ubc9. Angew Chem Int Ed Engl. 2016;55:5703–7.

42. Hirohama M, Kumar A, Fukuda I, Matsuoka S, Igarashi Y, Saitoh H, et al. Spectomycin B1 as a novel sumoylation inhibitor that directly binds to SUMO E2. ACS Chem Biol. 2013;8:2635–42.

43. Komiya M, Ito A, Endo M, Hiruma D, Hattori M, Saitoh H, et al. A genetic screen to discover sumoylated proteins in living mammalian cells. Sci Rep. 2017;7:17450–7.

44. Vertegaal AC, Andersen JS, Ogg SC, Hay RT, Mann M, Lamond AI, et al. Distinct and overlapping sets of SUMO-1 and SUMO-2 target proteins revealed by quantitative proteomics. Mol Cell Proteom. 2006;5:2298–310.

45. Brandt M, Szewczuk LM, Zhang H, Hong X, McCormick PM, Lewis TS, et al. Development of a high-throughput screen to detect inhibitors of TRPS1 sumoylation. Assay Drug Dev Technol. 2013;11:308–25.

46. Saitoh N, Uchimura Y, Tachibana T, Sugahara S, Saitoh H, Nakao M, et al. In situ sumoylation analysis reveals a modulatory role of RanBP2 in the nuclear rim and PML bodies. Exp Cell Res. 2006;312:1418–30.

47. Zlotkowski K, Hewitt WM, Sinniah RS, Tropea JE, Needle D, Lountos GT, et al. A small-molecule microarray approach for the identification of E2 enzyme inhibitors in ubiquitin-like conjugation pathways. SLAS Discov. 2017;22:760–6.

48. Liu B, Mink S, Wong KA, Stein N, Getman C, Dempsey PW, et al. PIAS1 selectively inhibits interferon-inducible genes and is important in innate immunity. Nat Immunol. 2004;5:891–8.

49. Sampson DA, Wang M, Matunis MJ. The small ubiquitin-like modifier-1 (SUMO-1) consensus sequence mediates Ubc9 binding and is essential for SUMO-1 modification. J Biol Chem. 2001;276:21664–9.

50. Yunus AA, Lima CD. Lysine activation and functional analysis of E2-mediated conjugation in the SUMO pathway. Nat Struct Mol Biol. 2006;13:491–9.

51. Mascle XH, Lussier-Price M, Cappadocia L, Estephan P, Raiola L, Omichinski JG, et al. Identification of a non-covalent ternary complex formed by PIAS1, SUMO1, and UBC9 proteins involved in transcriptional regulation. J Biol Chem. 2013;288:36312–27.

52. Erlanson DA. Introduction to fragment-based drug discovery. Top Curr Chem. 2012;317:1–32.

53. Desterro JM, Rodriguez MS, Kemp GD, Hay RT. Identification of the enzyme required for activation of the small ubiquitin-like protein SUMO-1. J Biol Chem. 1999;274:10618–24.

54. Desterro JM, Thomson J, Hay RT. Ubc9 conjugates SUMO but not ubiquitin. FEBS Lett. 1997;417:297–300.

55. Rodriguez MS, Dargemont C, Hay RT. SUMO-1 conjugation in vivo requires both a consensus modification motif and nuclear targeting. J Biol Chem. 2001;276:12654–9.

56. Hay RT. SUMO: a history of modification. Mol Cell. 2005;18:1–12.